J. Fluid Mech. (1993), *vol.* 250, *pp.* 253–276

Oscillatory instabilities produced by heat from a temperature-controlled hot wire below an interface

By C. ROZÉ, G. GOUESBET AND R. DARRIGO

Laboratoire d'Energétique des Systèmes et Procédés, URA CNRS no. 230, INSA de Rouen, BP 08–76131–Mont Saint Aignan Cedex, France

(Received 18 June 1990 and in revised form 25 November 1992)

New experimental results are reported for the motion of a liquid surface caused by the heat released from a hot wire below the surface. Starting from a base state with steady convection and steady deformation of the free surface caused by variations in surface tension and heat transport to the surface, the system loses its stability through a supercritical Hopf bifurcation occurring on a curve $f(\Delta T_*, d) = 0$ in which d is the distance between hot wire and surface and ΔT_* a critical temperature difference. These experiments are a model for more complex laser heating experiments in which chaotic motions may occur. Some emphasis is placed on the characterization of propagating waves produced on the surface after the occurrence of the bifurcation.

1. Introduction

The study of nonlinear dissipative dynamical systems has been a subject of increasing interest mainly since the discovery of the first strange chaotic attractor by Lorenz (1963). Among the relevant hydrodynamic instabilities, such as Rayleigh–Bénard and Bénard–Marangoni effects (Zierep & Oertel 1982), we have been interested in a phenomenon called thermal lens oscillations (TLOs) or optical heartbeats that we first described in Anthore *et al.* (1982) and then systematically investigated. TLOs may be produced when a laser beam propagates horizontally below a free surface, or vertically upwards, in an absorbing liquid (Gouesbet, Rhazi & Weill 1983; Gouesbet & Lefort 1987, 1988). They may exhibit various types of behaviour from equilibria and limit cycles up to chaos. These phenomena concern oscillations of luminous intensity of the laser beam leaving the cell, oscillatory convection inside the cell and oscillatory motion of the free surface. A systematic study of the characterization of chaotic motion generated by TLOs has been recently carried out (Meunier-Guttin-Cluzel 1990), leading us to the conclusion that data may be understood in terms of deterministic chaos with a small number of degrees of freedom. These results confirm a simple model by Gouesbet (1990*a*, *b*) in which observed phenomena are explained as a result of the coupling between a mechanical oscillator associated with the free surface and a thermal oscillator associated with the heating source. Recently, two other research teams have become interested in TLOs and associated phenomena such as the dynamics of laser-induced bubbles (Viznyuk & Sukhodol'skii 1988; Bazhenov *et al.* 1989*a*, *b*). These experiments are also good candidates for the study of hydrodynamic instabilities under microgravity conditions in space (Gouesbet & Sukhodol'skii 1991).

With the original purpose of a better understanding of the features described above, we designed similar experiments in which heating below the free surface is carried out using a hot wire (HWEs: Hot-Wire Experiments) instead of a laser (HBEs: HeartBeat

Experiments), allowing simpler and better-controlled experiments. After preliminary experiments with a power-controlled hot wire (Weill, Rhazi & Gouesbet 1982), systematic measurements have been carried out with a temperature-controlled hot wire (Weill, Rhazi & Gouesbet 1985; Gouesbet, Weill & Lefort 1986). The most important results are as follows. When ΔT (the difference between the temperatures of the hot wire and the ambient bath) is small, the system is steady. Above a critical $\Delta T = \Delta T_*$ depending on distance d between the hot wire and the free surface, convection in the liquid becomes oscillatory and we also simultaneously observe free-surface oscillations in the form of propagating waves. The onset of overstability at ΔT_* has up to now been characterized as a supercritical Hopf bifurcation. Oscillations appear with a vanishingly small amplitude at the bifurcation and with a well-defined fundamental frequency f_*. Critical values of ΔT_* and f_* have been measured for four silicon oils (47V5, 47V10, 47V50 and 47V100). Critical profiles $\Delta T_*(d)$ and $f_*(d)$ depend on the oil but, when appropriately presented in reduced forms, they collapse reasonably well to single profiles $\Delta T_*^+(d^+)$ and $f_*^+(d^+)$, where ΔT_*^+, f_*^+ and d^+ are dimensionless quantities (Gouesbet 1987). It has also been shown that there is a quantitative similarity between critical quantities for Hopf bifurcation in HBEs and HWEs (Gouesbet & Lefort 1988). Although no secondary instabilities have been observed up to now in HWEs for reasons which are not fully clarified, these HWEs provide us with a good experimental model of the Hopf bifurcation observed in HBEs.

To appreciate the originality of these HBEs and HWEs with respect to other classical temperature-driven hydrodynamical instabilities, it is of interest to point out some qualitative features which make them different to the overstability phenomena in the Rayleigh–Bénard–Marangoni convection observed when a temperature gradient is imposed vertically across a horizontally infinite liquid layer. The critical characteristics (critical temperature differences, critical frequencies, critical wavenumbers) at the onset of overstability have been investigated by Takashima (1981*a*, *b*) in the case of a pure Marangoni mechanism, with the conclusion that overstability can only set in when the rigid wall is cold (i.e. the free surface is hotter than the rigid heat source). This work has been recently complemented by the study of marginal overstability under simultaneous surface tension and buoyancy effects by Gouesbet & Maquet (1989), Gouesbet *et al.* (1990) and also later by Perez-Garcia & Carneiro (1991). The more complete case when surface tension, buoyancy and shear effects act simultaneously is discussed by Rozé, Gouesbet & Maquet (1990) and Gouesbet, Rozé & Maquet (1992). For standard liquids in which surface tension decreases when temperature increases and with a positive coefficient of volume expansion, the fact that overstability sets in only with a cold rigid wall is essentially confirmed, except for some restricted values of control parameters, i.e. for crispation numbers bigger than 0.015. Generally, it can be claimed that overstability is more unlikely with hot rigid walls than with cold rigid walls, although it is nevertheless possible. In contrast, in HBEs and HWEs, oscillatory motions generically occur when the free surface is heated from below, an essential qualitative difference with respect to the classical case of an infinite horizontal liquid layer. These last experiments therefore provide us with new examples of temperature-driven hydrodynamical instabilities which are very far from being fully understood.

The present paper reports new results for HWEs obtained after those published by Weill *et al.* (1982, 1985), and Gouesbet *et al.* (1986), using an improved experimental set-up. Instead of only studying silicon oils, the present work complements previous data by also investigating the critical quantities for the onset of oscillations in pentanol. Beside confirming our previously published results at marginality for silicon oils, the new results for pentanol at marginality produce new questions, and reveal that a

complete understanding of the observed phenomena could require much more skill than we expected. However, the most significant extensions concern the study of the domain $(\Delta T, d)$ beyond the critical line $f(\Delta T_*, d)$ of the supercritical Hopf bifurcation, and a more systematic characterization of the propagating wave oscillations. One of the most challenging issues for the future might be the understanding of the exact nature of these waves. Because they propagate above and parallel to the hot wire, they form a good candidate for an examination of monodimensional spatio–temporal chaos. In this spirit, some experiments are currently underway using a very long hot wire of length 60 cm (P. Bergé & M. Dubois, private communication).

The paper is organized as follows. Section 2 describes the new experimental set-up. Section 3 is devoted to qualitative observations while §4 quantitatively discusses the Hopf bifurcation. Section 5 is devoted to supercritical oscillations beyond the Hopf bifurcation. Although this paper is essentially devoted to experiments, we summarize in §6 our present theoretical understanding of the phenomena studied. Section 7 contains conclusions.

2. Experimental set-up

The experimental set-up is an improved version of the one described by Weill *et al.* (1985). The hot wire is again platinum of length $L = 3$ cm and diameter $D = 20$ μm. The ratio L/D is big enough to ensure that the temperature profile along the wire is essentially constant (Reimann 1973; Schorr & Gebhart 1970; Paranthoën & Petit 1979), making the problem two-dimensional in the base state. The electric resistivity is $10.6 \times 10^{-4} \Omega$/m at 273 K and the temperature coefficient is 3.92×10^{-3} K^{-1}. The wire is soldered on the tips of flexible prongs and adjustments are carried out by means of a micrometric pedestal described by Weill *et al.* (1985, figure 2). It is then immersed in a tank with temperature controlled by a thermostat (Weill *et al.* 1985, figure 1). Differences between this part of the set-up and the previous one are rather minor. They are an increase of the dimensions of the tank, which are now 17 cm (length), 12 cm (width) and 10 cm (height), a change of the material used which is now stainless steel rather than copper, and the fact that the fluid for temperature control no longer flows in the tank walls, to decrease the level of parasitic vibrations. Major differences concern data acquisition and processing techniques as described below.

The hot-wire temperature is controlled by means of a constant-temperature anemometer (CTA), TSI.1755. The CTA relies on the balance of a Wheatstone bridge involving a variable control resistor R_c (see figure 1, in Weill *et al.* 1985) which determines the temperature T_w of the wire. The relation $T_w(R_c)$ is obtained from prior calibrations which are repeated each time the wire is changed after accidental breaking.

Transient oscillatory behaviour may be provoked by perturbations such as spurious parasitic electric intensities due to a manual modification of the resistor R_c. Damping of these transients may be time-consuming. Such events were likely to occur in the previous experimental set-up because the hot-wire temperature was adjusted by manual manipulation of a bank of AOIP resistances. To solve this problem and to avoid artificial introduction of undue perturbations, temperature control is now monitored by a microcomputer (Zenith Z148). The chosen value of R_c is entered on the keyboard, leading to the activation of a bank of high-quality relays. R_c may be adjusted from 0 to 127.5Ω with a step of 0.5Ω, corresponding to T_w ranging from 0 to about 516 °C with a step of 3 K. This step is equal to the uncertainty in ΔT given in Weill *et al.* (1985).

A TSI-1755 box provides an electric tension ΔV which is a constant when the system

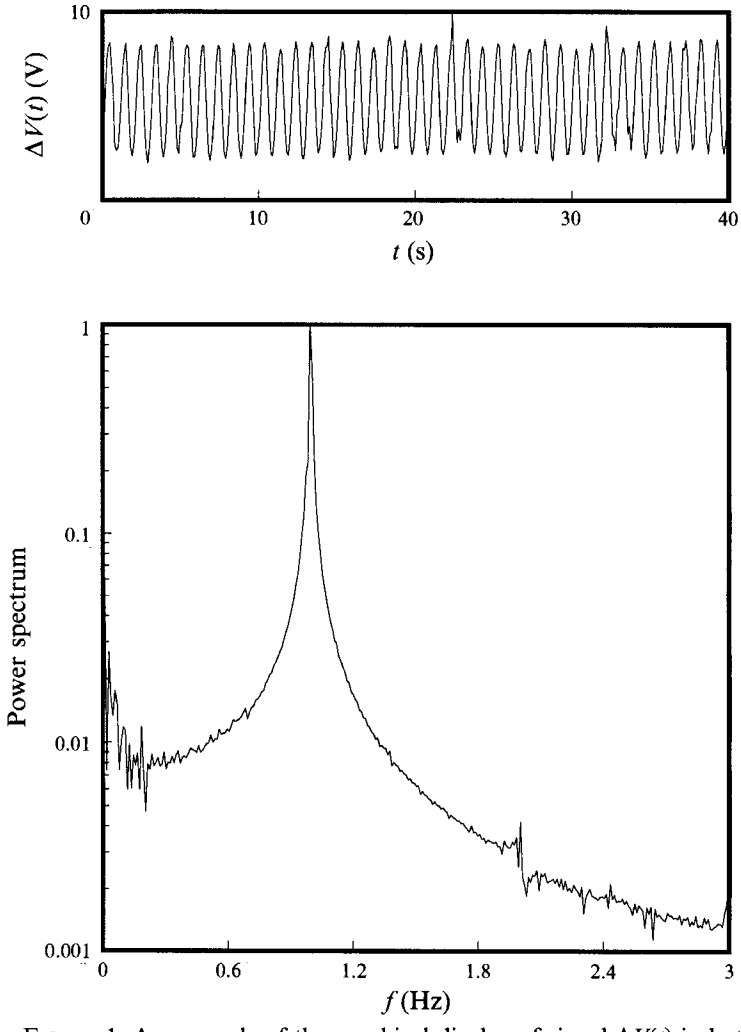

FIGURE 1. An example of the graphical display of signal $\Delta V(t)$ in both time and frequency domains.

is steady. When oscillatory instabilities occur, ΔV becomes time-dependent and is slaved to the oscillatory convection. In the experimental set-up of Weill *et al.* (1985), the signal ΔV was analysed using an FFT HP 3582 A spectrum analyser. In the present work, ΔV is amplified, sampled on 10 bits with a frequency which can be chosen in the range (3–1000 Hz) by means of a Data Translation DT2808 acquisition device installed in the computer, converted to integers and processed. To save time and allow for more comfortable on-line processing, the signal stored in the computer is read with a direct memory access (DMA) technique by a Turbo Pascal 4.0 computer program. The advantage of DMA is that computations may be carried out on a signal while, simultaneously, the acquisition device DT2808 goes on sampling and transferring data.

The $\Delta V(t)$ signal is consequently sampled at a frequency f_N and provides a sequence $\{x_i\}_{i=1}^n$ of n-values. These n-values are processed using a discrete FFT program computing the discrete Fourier transform of the sequence as defined by Bergé, Pomeau & Vidal (1984). The FFT algorithm requires $n = 2^p$ (p integer). In practice, we chose

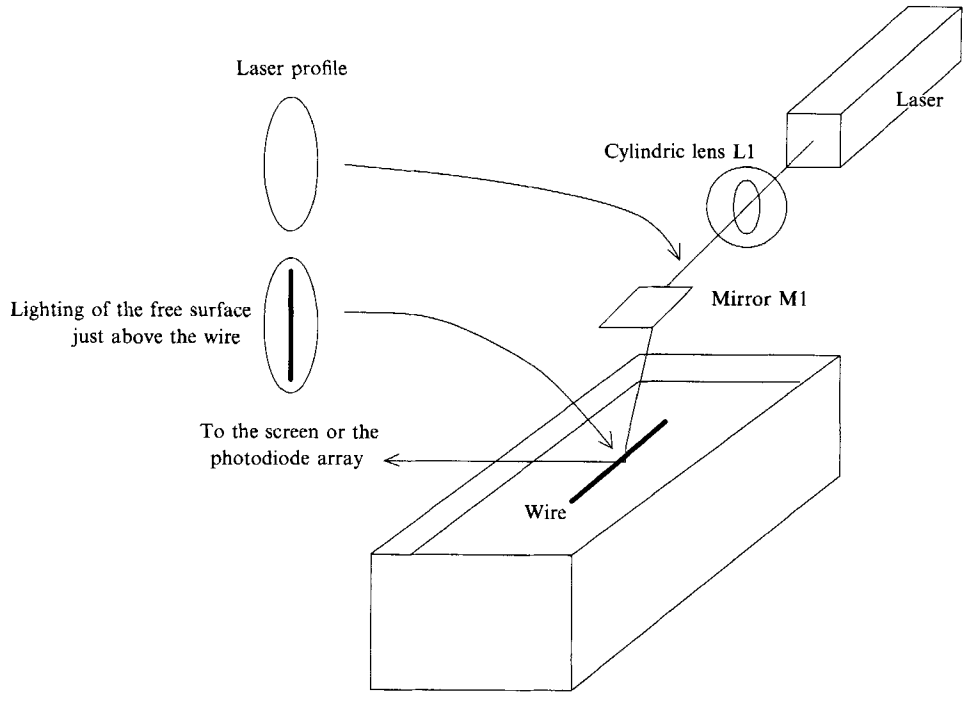

FIGURE 2. Experimental set-up for optical observations of the free surface.

$n = 1024$. The signal being real, all the information in the power spectrum is contained in only 512 points. The largest analysed frequency is $\frac{1}{2}f_N$ and frequency resolution is $\Delta f = f_N/1024$. We shall comment later on the relation between the cutoff frequency of the hot wire, more generally of the TSI-system, and the frequencies involved in the oscillatory motions studied.

Signals in the time and frequency domains may then be graphically displayed simultaneously on the computer screen. An example is shown in figure 1. The power spectrum is displayed on a logarithmic scale to let the reader appreciate the signal/noise ratio, which is of rather good quality. In order to speed up on-line processing, the computer is equipped with a numeric coprocessor 8087 and parts of computing and display programs are written in assembly language 8088. Thus, the signal can be continuously processed with a new graphical display appearing about every 15 s.

Finally, a last difference with the previous experimental set-up is the implementation of an optical technique as follows. Optical observations of the free surface are carried out by means of the set-up sketched in figure 2. An He–Ne laser beam of power 25 mW (small enough to avoid disturbing the system under study) is expanded into a large parallel beam and made into a light sheet by a cylindrical lens L1. Then it is projected onto the surface parallel to and just above the wire by mirror M1, i.e. the light sheet is parallel to the wire. The reflected light is then fed to a 1024-photodiode array or projected on to a screen by a mirror M2 and a lens L2 not shown on the figure. The photodiode array is illuminated by the image of the reflected sheet, the array and this image being parallel. This arrangement allows the characterization of wave characteristic lengths in the direction parallel to the wire.

The intensity received by each diode is digitized on 8 bits and the whole digitized

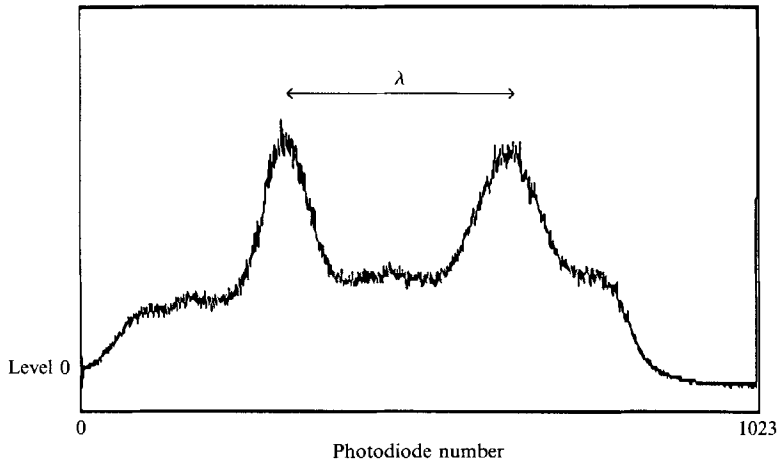

FIGURE 3. A photodiode array profile of free-surface waves.

image is fed on the computer and can be graphically displayed. An example is given in figure 3 showing how oscillation characteristic lengths λ may be determined.

3. Qualitative observations

3.1. *Hopf bifurcation*

To gain qualitative information on the nature of convection, we may observe on a screen after the tank the image of laser light crossing it, parallel to the wire through windows made in the sides.

When the difference ΔT between the hot-wire temperature T_w and the ambient bath temperature T_a is small, the system is steady (steady convection and steady deformation of the free surface). Although convection necessarily exists because ∇T is not parallel to the acceleration due to gravity $\boldsymbol{g}$ (Joseph 1976; Maquet, Gouesbet & Berlemont 1987), it is not significant at very small ΔT. Then, the laser light spot on the screen is essentially the same as when $\Delta T = 0$. At higher ΔT, convection becomes observable but still remains steady. The light spot evolves into two luminous wings, located symmetrically with respect to the wire. Although the image is perfectly motionless, the existence of regular convective motion in the cell is demonstrated by the motion of the shadows of particles introduced or naturally present in the liquid. Increasing ΔT again, we may finally observe (for a range of d) the appearance of oscillatory convection revealed by a regular and beautiful deformation of the luminous wings. Associated with this oscillatory convection, the electronic signal $\Delta V(t)$ from the TSI-1755 box also becomes oscillatory and optical observations using the system in figure 2 show oscillatory motion of the free surface taking the form of propagating waves. The transition from a steady to an unsteady state has been identified as a supercritical Hopf bifurcation arising at a critical $\Delta T_*(d)$ with a well-defined frequency f_*, but with vanishing amplitudes (from FFT spectra) and with characteristic free-surface oscillation lengths λ_* (from the photodiode array system). The vanishing character of the amplitudes is difficult to observe fully in the present work owing to the step of 3 K in adjusting the hot-wire temperature (§2) because the amplitudes evolve abruptly near the Hopf bifurcation threshold, but has been clearly observed by Gouesbet & Lefort (1988). An example of these hot-wire experiments is given in figure 4, showing

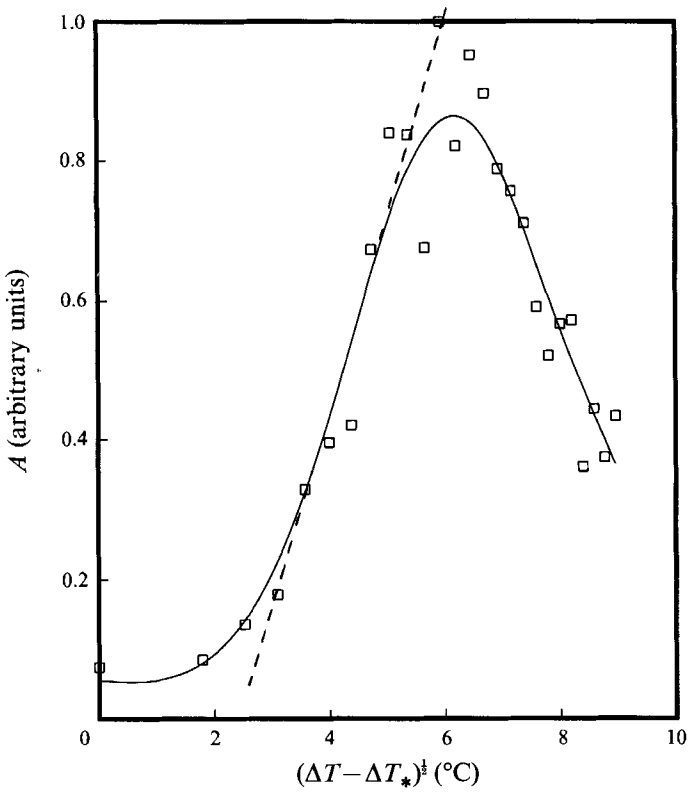

FIGURE 4. Amplitude (arbitrary units) versus square root of the distance from instability onset, $(\Delta T-\Delta T_*)$. Results are inaccurate for abscissa smaller than about 3. $\Delta T_* = 84$ °C.

amplitude A (arbitrary units) versus $(\Delta T-\Delta T_*)^{\frac{1}{2}}$. The continuous line is a manual fit. Since the accuracy of ΔT-measurements is typically 3 K, the amplitude A is not zero at $\Delta T = \Delta T_*$ in figure 4, as it should ideally be, because the measured ΔT_* used in the figure is not the true one but the ΔT nearest to ΔT_*. Also, accuracy of $(\Delta T-\Delta T_*)^{\frac{1}{2}}$ is then typically 2.5. Consequently, notwithstanding data in figure 4 for abscissa smaller than about 3, we observe that the oscillation amplitude scales like the square-root of the distance from instability onset in the vicinity of the bifurcation (see the dashed straight line) as it would for the behaviour of a supercritical Hopf bifurcation in normal form (Guckenheimer & Holmes 1983; Thomson & Stewart 1987). Similarly, we shall also observe later that frequency variations versus $(\Delta T-\Delta T_*)$ are linear in the vicinity of the bifurcation (figures 9, 12(*a*) and 14(*a*)), a behaviour which actually extends far beyond the bifurcation threshold.

On increasing ΔT again, no secondary instabilities are observed, in contrast with laser experiments (Gouesbet & Lefort 1988). According to a simple model (Gouesbet 1990*a*, *b*), we first believed that this resulted from holding the temperature of the hot wire at a constant value, leading to a phase space of dimension 2 in which secondary instabilities could not develop due to topological constraints. However, we may also argue that, even if the temperature is constant in the hot wire (a 1D-singular line embedded in a 3D-fluid), it is allowed to change in a 3D-neighbourhood of it. Therefore the behaviour of HWEs and HBEs should be similar. We shall return to this point in §5.1.

3.2. *Steady deformation of the free surface*

Deformation of the free surface is investigated using the photodiode array system. At small ΔT, when convection is not significant, the free surface remains plane. When ΔT increases, we then observe a steady deformation which takes the form of a crest or a trough. The trough is produced when distance d is small. On a screen replacing the photodiode array, we observe a thin luminous strip, demonstrating the concentration of light rays. This is typical of a surface tension mechanism. Conversely, when d is large, the screen shows a dark strip between two parallel bright strips, demonstrating the existence of a crest, typical of a buoyancy mechanism (Kayser & Berg 1973). Photographs of the light distribution on the screen replacing the diode array are shown in both cases in figure 5(a, b) respectively. Somewhere in between, for a $d \approx d_{\min}$, the two mechanisms cancel and the surface is again essentially plane. Intuitively, this is the most favourable condition for oscillation growth, qualitatively explaining why the critical ΔT_* exhibit a minimum for $d = d_{\min}$. In fact, the conflict between crests and troughs has been recently invoked to explain why buoyancy in the bulk is an efficient inhibitor of overstability in Marangoni-driven instabilities for a horizontally infinite liquid layer (Gouesbet *et al.* 1990), although a complementary study of the same problem by Perez-Garcia & Carneiro (1991) with other parameter values revealed that this inhibiting character is not so general as we may have thought.

3.3. *Free-surface oscillations*

Increasing ΔT again, free-surface oscillations appear at $\Delta T_*(d)$ in the form of propagating waves. Similarly to figure 5(a, b) under steady conditions, figure 5(c) exhibits a screen image of the free-surface waves under oscillatory conditions.

In some cases, the waves emerge above one end of the wire and propagate along the surface, parallel to the wire, to die out at the other end. We believe that this situation arises when the surface is not perfectly horizontal, resulting in the lack of symmetry in wave propagation. In such cases, FFT spectra essentially contain a single peak indicating a pure sinusoidal waveform ΔV (see the example in figure 1). In other cases, presumably when the surface is nearly perfectly horizontal, oscillations appear above the centre of the hot wire and split into two waves, propagating in opposite directions towards the ends of the wire. Each wave, starting from the same point, may not then vibrate at exactly the same frequency, leading to signals reminiscent of quasi-periodicity. In this configuration, we may also observe some signals reminiscent of intermittency. Indeed, the two-wave regime is difficult to reproduce and lacks stability. When oscillations start in this two-wave regime, they generally settle down after a more or less long transient to the first single-wave regime defined by a single frequency, as in figure 1. Infra-red photographs clearly demonstrate that the effect of these waves is to abruptly transport the heat from the wire to the surface, a qualitative fact which inspired the aforementioned simple model (Gouesbet 1990a, b). These infra-red observations are particularly convincing with very viscous liquids like diethylphtalate. They show bright spots corresponding to high-temperature domains which are disrupted by the formation of waves.

The time delay between switching on of the wire temperature T_w and the appearance of oscillations (for T_w big enough) is very dependent on distance d and on liquid viscosity. For viscous liquids and large d, it can be as large as 20 min. Conversely, for small viscosities and small d, it is virtually zero. Once oscillations have developed, they are remarkably stable and may be observed for at least a day with constant amplitude and frequency. When the electric supply to the wire is switched off, the waves disappear

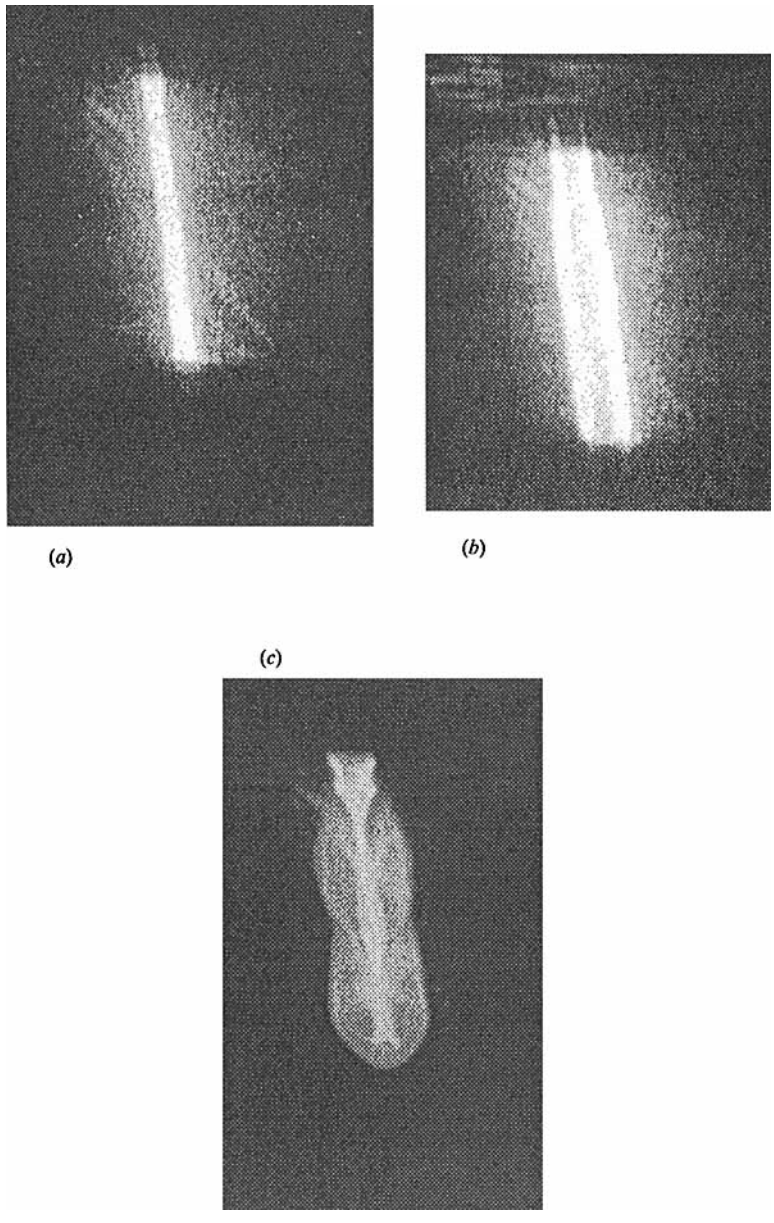

FIGURE 5. Photographs of the light distribution on the screen replacing the iode array: (*a*) *d* small, (*b*) *d* large, (*c*) oscillatory motion.

immediately without any observable relaxation time. This is in contrast to capillary and gravity waves which could be more progressively damped and would still propagate for a while after the agency of their creation has disappeared.

Another behaviour of the waves to mention concerns their interaction with solid obstacles located in their path between the ends of the wire. Apart from single-peak spectra like in figure 1, we may also observe spectra with harmonics of smaller amplitudes. The presence of a dust particle or a bubble trapped in the trough of the surface or stuck to the wire leads to spectra with several frequencies, in which

	Silicon oil	Pentanol-1
Kinematic viscosity	ν (m²/s) 10×10^{-6}	5.43×10^{-6}
Specific mass	ρ (kg/m³) 930	814.8
Thermal conductivity	λ (W/(m K)) 0.13	0.144
Specific heat	C_p (kJ/(Kg K)) 1.88	3.15
Surface tension	σ (N/m) 20.1×10^{-3}	25.6×10^{-3}
Thermal diffusivity	a_T (m²/s) 7.435×10^{-8}	5.610×10^{-8}
Expansion factor	α_v (K^{-1}) 1.0×10^{-3}	0.868×10^{-3}
Rate of variation of the surface tension with temperature	$\frac{d\sigma}{dT}$ (N/(m K)) -0.07×10^{-3}	-0.088×10^{-3}

TABLE 1. Thermophysical properties of silicon oil 47V10 at 25 °C; and pentanol-1 at 20 °C

harmonics may be stronger than the fundamental frequency. However, waves seemingly are not altered permanently by obstacles located on their way. For instance, we located a metallic wire on the path separating the double-convection annular eddy, followed by the waves. Optical observations show that waves may be strongly deformed by the obstacle, but are rebuilt behind it without any reflection from it. From such qualitative observations, we wonder whether these waves might be solitons (or solitary waves) canalized by convection rolls. In any case, these propagating waves are worth specific experiments to identify their exact nature and systematic investigations are planned. We must here repeat that companion experiments using a long hot wire of length 60 cm are currently running (P. Bergé, M. Dubois, private communication) and should produce new insights into the exact nature of these waves, still mysterious to us.

3.4. *Choice of liquids*

Several liquids have been qualitatively tested. Some develop oscillations (benzene, silicon oils, toluene, pentanol, di(ethyl-2 hexyl)phtalate) while others do not (water, acetone, ether, ethanol, cyclohexane, n-hexane). Up to now, we do not have a good explanation for this difference of behaviour which however must depend on dimensionless or even dimensional groups of thermophysical properties. The simple model described by Gouesbet (1990*a*, *b*) cannot directly help because it produces universal results in which all thermophysical properties are eliminated.

For useful experiments, the liquid must not be too volatile, its boiling temperature must be high enough and its viscosity not too large. Also, it must be chemically inert with respect to the wire, wire supports and tank materials and its toxicity preferably null or at least small. These conditions severely limit the opportunities. Quantitative studies have been mostly carried out with a silicon oil 47V10 (previously used by Weill *et al.* 1985). Silicon oils, complying with the above requirements, appear to be an ideal liquid for HWEs. Some other quantitative experiments have been carried out with pentanol. Although this liquid is volatile, it reacts quickly to thermal constraints, permitting the duration of experiments to be limited and the diminution of the surface height due to vaporization to be neglected. Mass transfer at the surface might however constitute an extra source of instability. Thermophysical properties for silicon oil 47V10 and pentanol are displayed in table 1.

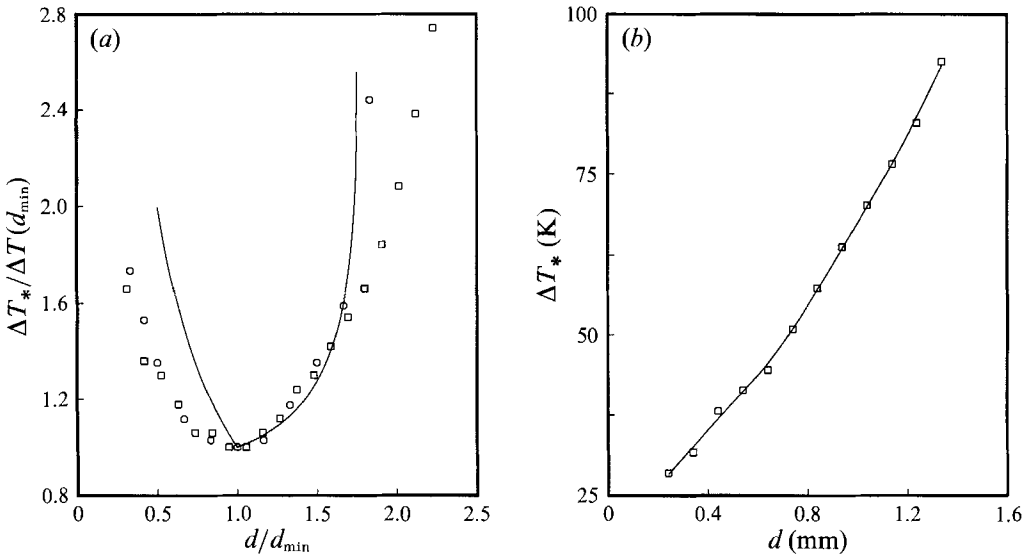

FIGURE 6. (*a*) Critical temperature difference ΔT_* versus distance d expressed in reduced forms $\Delta T_*/\Delta T_*(d_{\min})$ versus $d/d_{\min}$ for silicon oil 47V10: □, present results; ○, Weill *et al.* (1985); continuous line, Gouesbet's model. (*b*) Critical temperature difference ΔT_* versus d for pentanol.

4. Critical characteristics for Hopf bifurcation

Control parameters are the temperature difference ΔT (with ambient bath temperature fixed at T_a) and distance d.

4.1. *Critical temperature differences* ΔT_*

To determine the critical curve $f(\Delta T_*, d) = 0$ in the control parameter plane, a distance d is chosen and hot-wire temperature is fixed at a T_w at which we are sure that the state is asymptotically steady. T_w is afterward progressively increased by small increments and, at each step, the system is observed for a time long enough to be sure that no perturbation is amplified to produce oscillatory behaviour. The temperature T_w at which oscillatory behaviour is marginally observed determines ΔT_*.

In some experiments, we also proceeded by starting from a large ΔT for which oscillatory motion is asymptotically observed and decreasing T_w to recover a steady motion in the liquid and a steady deformation of the surface. Within an accuracy of about 3 K (the smallest temperature increment allowed by our automatic temperature control system), we find identical ΔT_* for each procedure, confirming that the bifurcation is essentially supercritical. At high d we detected a small amount of subcriticality (hysteresis) which might be however attributed to an increase of the delay required to completely kill transients.

When d is increased from a value $d_{\min}$, ΔT_* also increases. The biggest d value that we may investigate is then limited by the liquid boiling temperature. Also, small bubbles are formed which may stick to the wire or to the surface, preventing accurate measurements. We note that the formation of bubbles is a parasitic event in this context, but it can be studied in its own right (Bazhenov *et al.* 1989*b*). At small d, the limit is imposed by the diameter of the wire which may mechanically interact with the surface.

For silicon oil 47V10, critical $\Delta T_*(d)$ values are displayed in figure 6(*a*) ($T_a = 28$ °C), in the reduced form $\Delta T_*/\Delta T_*(d_{\min})$, versus $d/d_{\min}$, where $d_{\min}(1.0\text{ mm})$ is the distance

d at which ΔT_* has a minimum $\Delta T_*(d_{\min})$, here equal to 54 °C. We also include results of Weill *et al.* (1985) showing a good agreement. In their experiments, the values for $d_{\min}$ and $\Delta T_*(d_{\min})$ were 1.2 mm and 34 °C respectively, the differences being attributed to a modification of the bath temperature which was set to 25 °C, and also perhaps to different contamination of the interface. The reduced data in figure 6 agree well with results from Gouesbet's model (1990*a*, *b*) shown as a continuous line.

For pentanol, ΔT_* versus d is given in figure 6(*b*). The most striking difference with silicon oil is the absence of any $d_{\min}$, preventing us from presenting the results in reduced forms as in figure 6(*a*). The absence of a $d_{\min}$ value has also been reported in experiments with toluene, in which the power supplied to the wire was controlled instead of the temperature (Weill *et al.* 1982). We first tried to define a fictitious $d_{\min}$ in pentanol experiments by assuming that pentanol results satisfied the reduced profile of figure 6(*a*) and that only the right increasing branch of this profile could have been measured. We found a negative $d_{\min} = -0.6$ mm, a result which cannot be accepted on physical grounds. At this stage, we must then conclude that either $d_{\min}$ does exist but the reduced profile of silicon oil experiments and Gouesbet's model is not satisfied in pentanol and toluene experiments, or that $d_{\min}$ does not exist. In figure 6(*b*) measurements are again limited by boiling temperature at large d while they are mechanically limited by the wire diameter at small d.

Such limitations at small d do not exist in HBEs. Recent experiments in HBEs with toluene (Meunier-Guttin-Cluzel 1990) did show the existence of a $d_{\min}$ when the laser beam is very close to the surface, actually interacting with it in a meniscus region near the wall of the HBE-cell. Such a $d_{\min}$ cannot be observed in HWEs but, very likely, virtually exists. Therefore, the reduced profile of silicon oils observed in experiments (Gouesbet 1987; Gouesbet & Lefort 1988) and in Gouesbet's (1990*a*, *b*) model is not satisfied by toluene and pentanol. We emphasize that Gouesbet's model presents theoretical results in terms of reduced quantities in which all thermophysical properties are eliminated, and that no *ad hoc* effort was carried out to attempt to fit silicon oil results, i.e. the agreement between silicon oil data and Gouesbet's model has a physical meaning and does not result from forcing the model to fit silicon oil data.

This difference of behaviour of toluene and pentanol could be attributed to the additional complexity for volatile liquids due to the effect of mass transfer through the interface. However, this explanation is not likely to be correct because toluene experiments in HBEs are carried out in small cells which are sealed, preventing mass transfer through vaporization except for a small transient time. Therefore, understanding the pentanol experiments in this paper definitely demands a new theoretical effort. Let us however remark that, if a $d_{\min}$ virtually exists, then pentanol experiments are still in qualitative agreement with Gouesbet's model although the quantitative agreement for the ΔT_*-values is lost.

4.2. *Frequencies f_1,f_2 and critical frequencies f_**

Frequencies f_1 are measured from the ΔV-FFT signal (§2), tracking oscillatory convection around the wire. Simultaneously, we measured frequencies f_2 by Fourier transforming a signal obtained from one photodiode of the photodiode array, tracking oscillatory motion of the surface. A set of comparisons between f_1 and f_2 has been obtained for various ΔT and d, leading to $f_1 = f_2 = f$ demonstrating the strong coupling between oscillatory convection and oscillatory motion of the free surface. We furthermore remark that there is virtually no cutoff frequency associated with f_2-measurements, although a cutoff frequency does exist for the f_1 owing to the limited hot-wire response and also to the TSI-box. For a tungsten wire of diameter 4 μm in air,

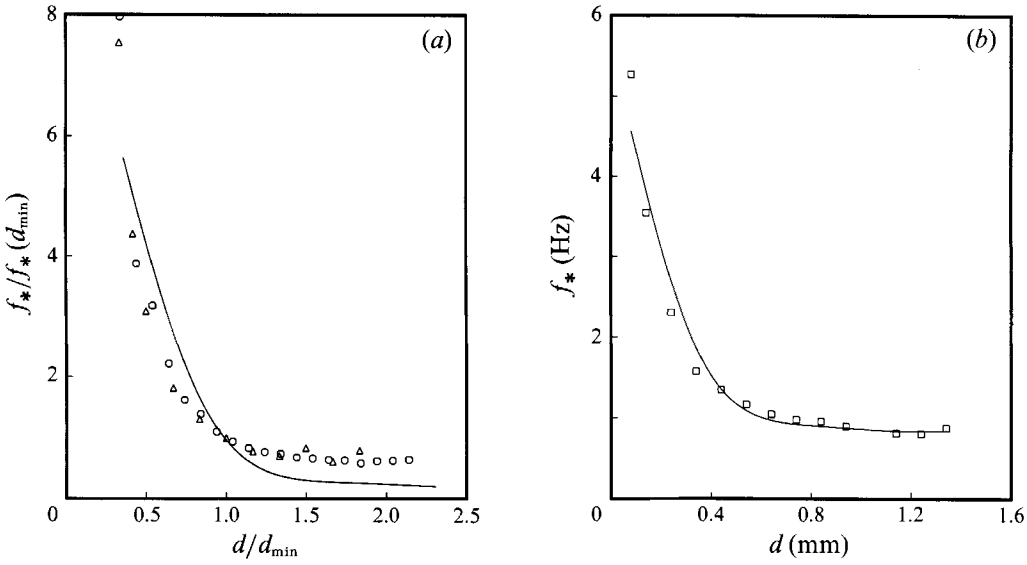

FIGURE 7. (*a*) Critical frequency f_* versus d expressed in reduced forms $f_*/f_*(d_{min})$ versus d/d_{min} for silicon oil: ○, present results; △, Weill *et al.* (1985); continuous line, Gouesbet's model. (*b*) Critical frequency f_* versus d for pentanol.

the cutoff frequency of the whole system is 25 Hz. Although our experiments are operating under different conditions, we estimate that the response time of the system is significantly faster than the characteristic times of the phenomena studied. The agreement between f_1 and f_2 provides an indirect confirmation of this. Ideally, it would also be interesting to compute cross-spectra and the coherence between the f_1- and f_2-signals, providing information about the phase difference between the surface motion and the wire temperature as a function of frequency. This phase difference would be related to a characteristic time of heat transfer between the wire and the free surface and might presumably provide us with some experimental knowledge about the heat transfer mechanisms. Unfortunately, such information is not accessible with the present experimental set-up because, owing to microcomputer limitations, f_1- and f_2-signals cannot be simultaneously recorded. This issue might be solved in future experiments.

Critical f_* values for silicon oil ($T_a = 28$ °C) are displayed in figure 7(*a*) as $f_*/f_*(d_{min})$ versus d/d_{min}, with $f_*(d_{min}) = 1.25$ Hz. The continuous line comes from Gouesbet's (1990*a*, *b*) model showing good agreement. There is also good agreement with Weill *et al.*'s (1985) data shown in figure 7(*a*). In this last study, $f_*(d_{min}) = 0.65$ Hz. Comments concerning this difference for $f_*(d_{min})$ would be similar to those made in §4.1 for the differences for d_{min} and $\Delta T_*(d_{min})$. Furthermore, f_* significantly changes when d becomes smaller than $d \approx d_{min}$. Therefore, a difference in d_{min}-values leads to a significant difference in $f_*(d_{min})$. Results for pentanol are given in figure 7(*b*) ($T_a = 24$ °C). In contrast with the ΔT_*-results, profiles in figure 7(*a*, *b*) look (at least qualitatively) similar. Therefore, because f_*-measurements presented in reduced form in figure 7(*a*) for silicon oils quantitatively agree with Gouesbet's (1990*a*, *b*) model, results in figure 7(*b*) for pentanol also qualitatively agree with the model. We now discuss critical characteristic lengths λ_* which cannot be predicted by Gouesbet's model.

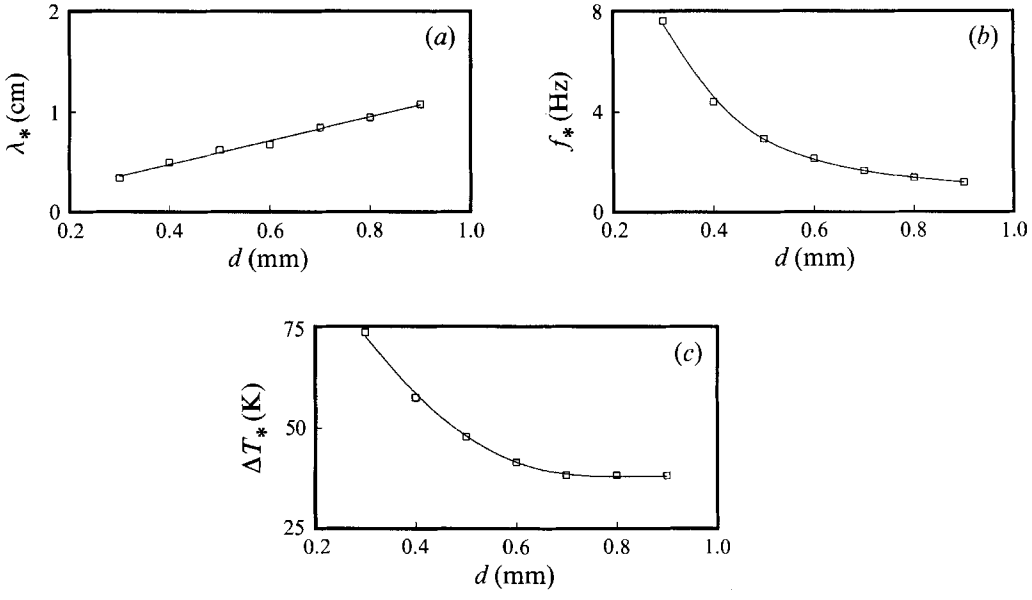

FIGURE 8. Simultaneous measurements of critical characteristic lengths λ_*, critical frequencies f_* and critical temperature differences ΔT_* versus d for silicon oil.

4.3. *Critical characteristic lengths* λ_*

We define a characteristic length λ as the distance between two identical luminous structures (see figures 3 and 5*c*). The exact status of these characteristic lengths depends on the nature of the waves. We may think that these lengths are not exactly proper wavelengths but are, rather, related to distances between two consecutive solitary waves. Experiments currently underway on a 60 cm hot wire (P. Bergé, M. Dubois, private communication) show that the train of waves propagates regularly (at least under certain circumstances) along the whole length of the wire, and suggest that we may be faced with a more or less classical wave, in which case λ would be a proper wavelength. At present, we are not able to decide whether free-surface oscillations form a single wave or a train of self-organized solitary waves. However, in any case, λ may be evaluated from the photodiode array signal by counting the number of pixels between two identical structures or from video movies, leading to nearly identical results. In both cases, the lengthscale is given by the length of the wire.

Results are shown at marginality ($\lambda = \lambda_*$) for silicon oil ($T_a = 27$ °C) in figure 8(*a*). We observe that λ_* increases proportionally to d, with $\lambda_* \approx 10d$. For d larger than about 1 mm, λ_* is larger than about 1 cm. This compares with the length of the wire, 3 cm, and so prevents us from correctly evaluating λ_* when d is too large because (i) waves do not travel far enough to become stationary, and (ii) they are deformed when they approach the ends of the wire.

Figure 8(*b*, *c*) also simultaneously displays critical f_* and ΔT_* for the same range of d as in figure 8(*a*). These results being for $T_a = 27$ °C, comparisons with the case of figures 6(*a*) and 7(*a*) ($T_a = 28$ °C) for which $\Delta T_*(d_{min}) = 54$ °C and $f_*(d_{min}) = 1.25$ Hz exemplify the sensitivity of the results to T_a when non-reduced values are used. They also support our comments concerning comparisons with results by Weill *et al.* (1985) given in §§4.1 and 4.2.

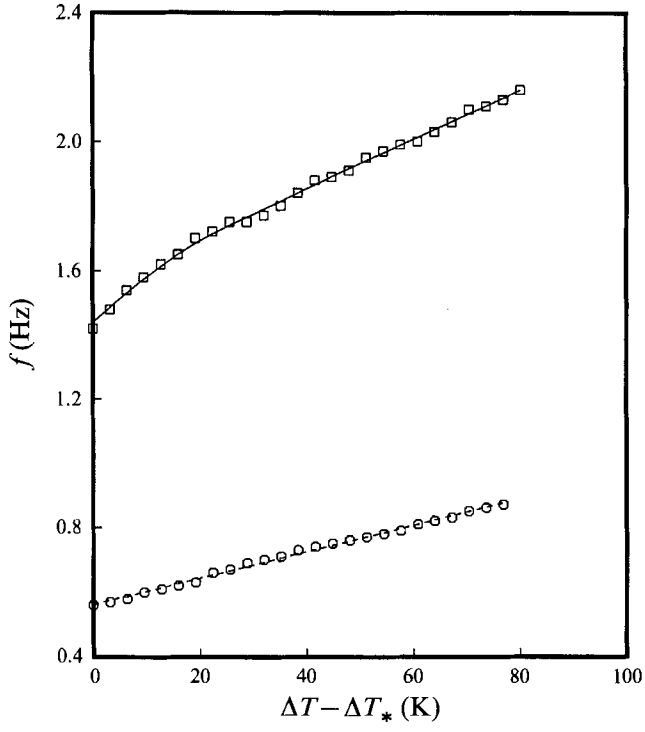

FIGURE 9. Frequency f versus $(\Delta T - \Delta T_*)$ for silicon oil, for two values of distance d: ——, $d = 0.76$ mm, $\Delta T_* = 57$ K; – – –, $d = 1.70$ mm, $\Delta T_* = 67$ K.

5. Supercritical oscillations

While only the critical quantities ΔT_* and f_* were discussed by Weill *et al.* (1985), they also presented results in the supercritical domain inside the marginal curves $f(\Delta T_*, d) = 0$. We successively consider the evolution of frequencies $f(\Delta T, d)$ and of characteristic lengths $\lambda(\Delta T, d)$ from which we may obtain a dispersion relation $\omega = f(k)$ in which $\omega = 2\pi f$ is the pulsation and $k = 2\pi/\lambda$ is a wavenumber.

5.1. *Supercritical frequencies*

For silicon oil 47V10, figure 9 displays f versus $(\Delta T - \Delta T_*)$ for two values of d. Measurements have been carried out at d fixed and increasing ΔT. Frequency increases steadily but slowly with ΔT. In the vicinity of bifurcation, i.e. at small values of $(\Delta T - \Delta T_*)$, f varies proportionally to the difference between $(\Delta T - \Delta T_*)$ and the threshold value for the onset of instability (see a similar comment in §3.1), a result which is also valid for the later figures 12(*a*) and 14(*a*). In all these figures, the linear increase extends far beyond the onset of instability except in figure 9 for the smallest value of d.

In order to compare the present HWEs with HBEs (Gouesbet & Lefort 1988), figure 10 displays supercritical frequencies f versus temperature differences ΔT (for HWEs) or laser power P (for HBEs) in terms of reduced quantities. There is qualitative similarity between both kinds of experiment in the supercritical domain beyond Hopf bifurcation. However, we also observe that the range of thermal driving constraint in HWEs $(\Delta T/\Delta T_*(d_{\min})$ up to $\approx 3)$ is much smaller than in HBEs $(P/P_*(d_{\min})$ up to $\approx 7)$. This difference in the investigated ranges is attributed to the fact that HWEs were carried out at atmospheric pressure while HBEs were carried out in a small sealed spectroscopic

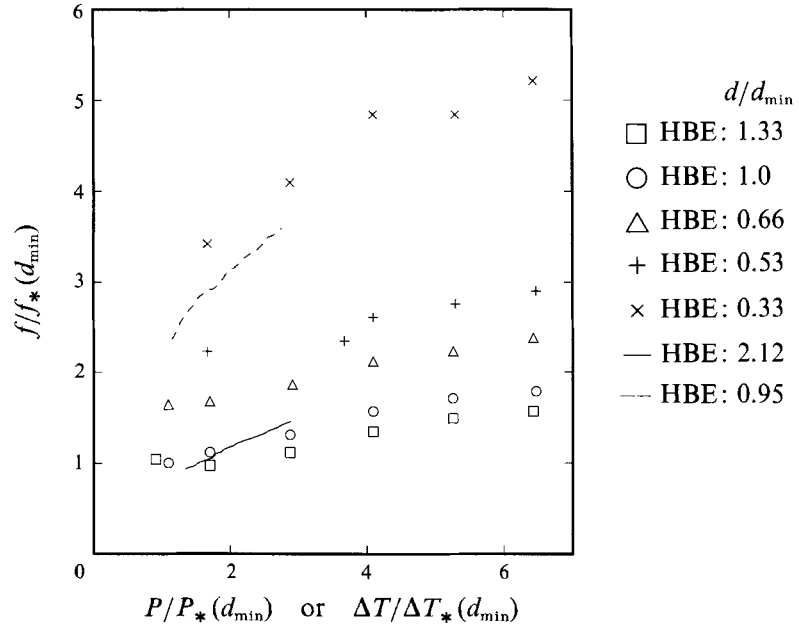

FIGURE 10. Reduced frequency $f/f_*(d_{min})$ versus reduced temperature difference $\Delta T/\Delta T_*(d_{min})$ for the hot-wire experiment (HWE) and versus reduced laser power $P/P_*(d_{min})$ (HBE).

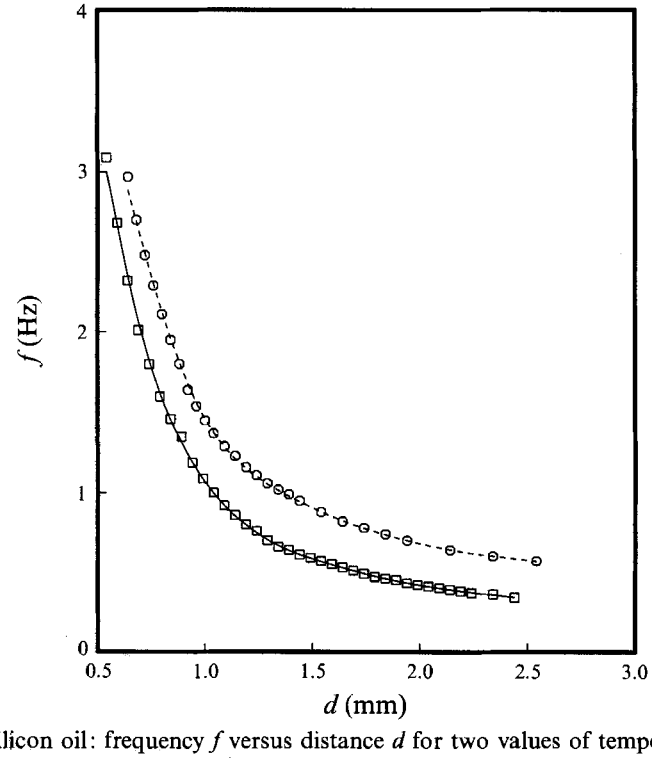

FIGURE 11. Silicon oil: frequency f versus distance d for two values of temperature difference ΔT: ——, $\Delta T = 33.5$ K; – – – –, $\Delta T = 97.5$ K.

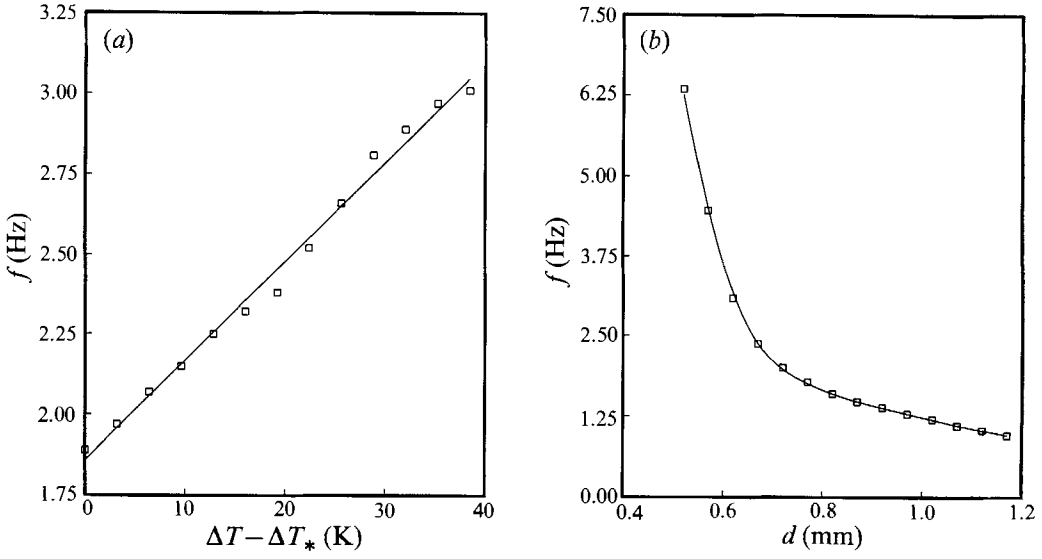

FIGURE 12. Pentanol: (*a*) f versus $(\Delta T-\Delta T_*)$; ——, $\Delta T_* = 50.9$ K; (*b*) f versus d.

cell in which pressure and therefore boiling temperature could increase at higher values.

Now, we commented at the end of §3.1 that no secondary instability is observed in HWEs beyond the Hopf bifurcation, in contrast with the case of HBEs. Although the temperature at the heating location is fixed in HWEs while it is allowed to float in HBEs, we also remarked that the behaviour of HWEs and HBEs should nevertheless be similar. This statement is partially confirmed by new HWEs currently underway in which the current intensity in the wire is fixed rather than the temperature. With the current intensity fixed, the temperature is now allowed to float at the heating location, similarly to HBEs. Although these new HWEs are far from complete, it happens that up to now secondary instabilities are still lacking. Figure 10 may provide us with a clue to understand the reason why. From Gouesbet & Lefort (1988, figure 8), we observe that secondary instabilities start at $P/P_*(d_{\min}) \approx 2$. Therefore, a likely reason for the lack of secondary instabilities in HWEs might be too small a range of $\Delta T/\Delta T_*(d_{\min})$ investigated. New experiments are planned to check this suggestion and the aforementioned working assumption. In such HWEs, it would be necessary to allow the pressure in the gas above the free surface to be controlled at values much bigger than atmospheric pressure. The implementation of such a control is however in practice very far from obvious.

Figure 11 displays f versus d for two values of ΔT, showing a rather hyperbolic decrease. Results in figures 9 and 11 may be approximately fitted by the following law:

$$f = \frac{A\Delta T + B}{d^{\frac{3}{2}}}, \tag{1}$$

representing a linear increase with respect to ΔT at d fixed (figure 9) and a hyperbolic decrease with respect to $d^{\frac{3}{2}}$ at ΔT fixed (figure 11), leading to f^2 approximately proportional to $1/d^3$.

Observations with pentanol are similar. Figure 12(*a*) displays f versus $(\Delta T-\Delta T_*)$ for $d = 0.46$ mm. Linearity is very good. Figure 12(*b*) displays f versus d for $\Delta T =$ 57 °C, leading again to a rather hyperbolic profile.

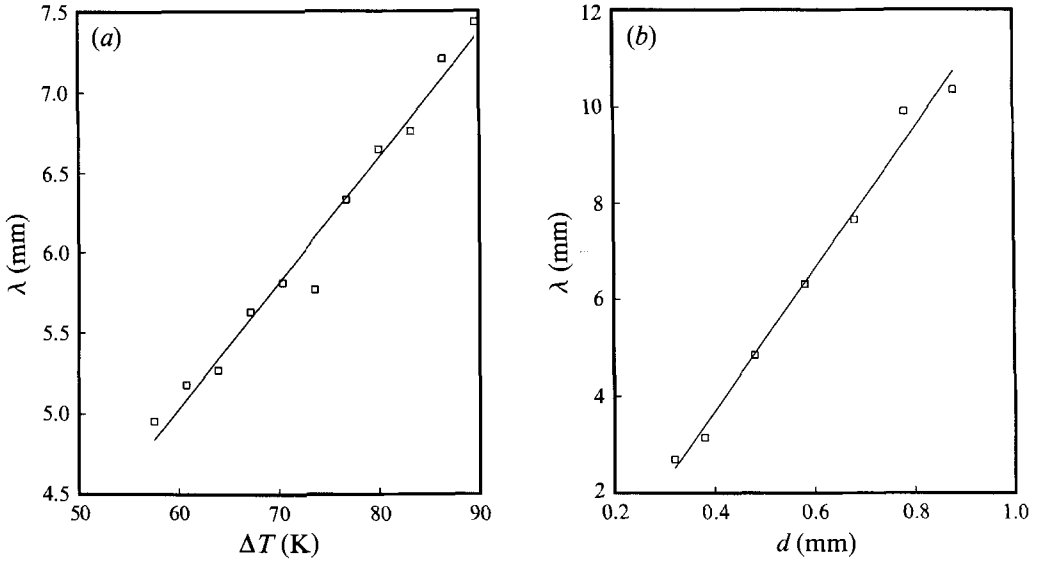

FIGURE 13. Silicon oil: (*a*) characteristic length λ versus ΔT; (*b*) characteristic length λ versus d.

5.2. *Supercritical characteristic lengths*

For silicon oil, figure 13(*a*) shows that λ increases linearly with ΔT for d fixed ($d = 0.80$ mm) and figure 13(*b*) that it also increases linearly with d for ΔT fixed ($\Delta T = 95$ °C). Then, supercritical characteristic lengths λ may be approximately fitted by

$$\lambda = C\Delta T d + Dd + E\Delta T + F. \tag{2}$$

Measurements could not be carried out with pentanol because characteristic lengths were not small enough with respect to the wire length.

5.3. *Dispersion relation*

To obtain accurately the constants A–F involved in relations (1) and (2), extensive measurements have been carried out in silicon oils. They are displayed in figure 14(*a*, *b*). Here, f and λ were simultaneously measured (conversely to experiments in §§ 5.1 and 5.2) to provide more accurate values of the constants. After linear regressions, we may rewrite (1) and (2) as

$$f = \mathscr{A}/d^{\frac{3}{2}}, \tag{3}$$

$$\lambda = \mathscr{B}d - \mathscr{C}, \tag{4}$$

with

$$\mathscr{A} = 0.01\Delta T + 0.67, \tag{5}$$

$$\mathscr{B} = 0.315\Delta T + 10.3, \tag{6}$$

$$\mathscr{C} = 0.090\Delta T + 2.44, \tag{7}$$

in which d is expressed in mm, ΔT in K, f in Hz and λ in mm.

Combining relations (3) and (4), we obtain

$$\omega \approx \frac{ak^{\frac{3}{2}}}{(1+bk)^{\frac{3}{2}}}, \tag{8}$$

in which a and b are constants.

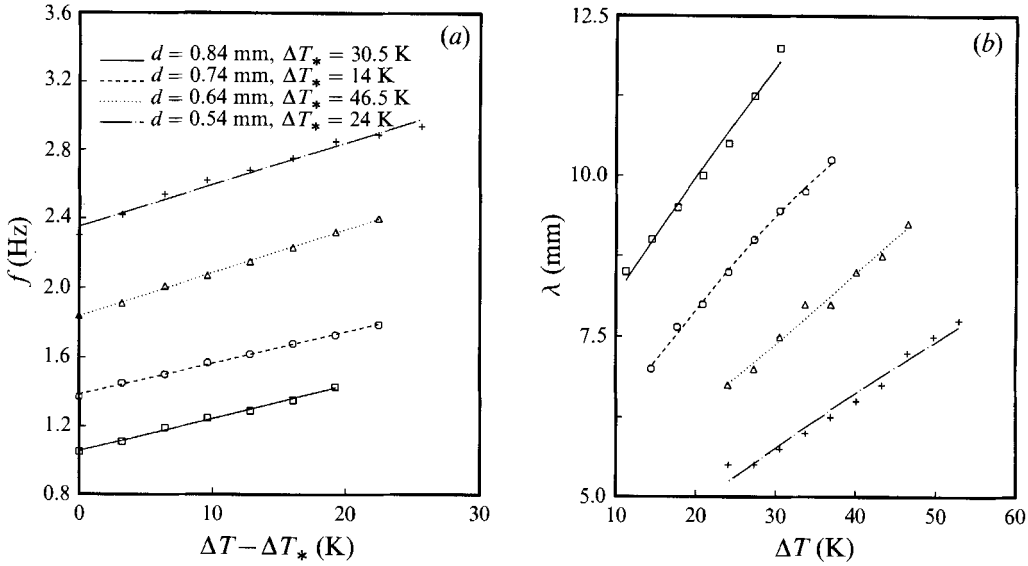

FIGURE 14. Silicon oil: (*a*) extensive measurements of f versus $(\Delta T - \Delta T_*)$, for several values of d; (*b*) extensive measurements of λ versus ΔT, for the same d values as in (*a*).

In the cases of capillary waves and gravity waves, the dispersion relations are $\omega \approx k^{\frac{3}{2}}$ and $\omega \approx k^{\frac{1}{2}}$ respectively (Landau & Lifshitz 1971). We therefore must conclude that the waves in these experiments are of a different nature. Our discussion in the introduction concerning differences between HWEs, HBEs, and the classical geometry of an infinite horizontal liquid layer reinforces the feeling that we are faced to a different family of surface waves and that the exact nature of these waves still remains to be elucidated, a fact that we have previously mentioned several times. We wonder whether they could be solitary waves or even solitons. There is current interest in the theoretical and experimental study of micro-solitons associated with surface tension phenomena. See for instance Garcia-Ybarra, Castillo & Velarde (1987) or Garcia-Ybarra & Velarde (1987). The theoretical analysis of such phenomena requires the introduction of nonlinearities, in contrast with the linear analysis results quoted in the introduction (Takashima 1981*a*, *b*; Gouesbet & Maquet 1989; Gouesbet *et al.* 1990; Perez-Garcia & Carneiro 1991; Rozé *et al.* 1990). In Garcia-Ybarra *et al.* (1987), for the classical case of a horizontal liquid layer, a new time and space nonlinear evolution equation of an air–liquid upper interface is derived, for thermocapillary flow in the absence of bulk buoyancy, generalizing the celebrated Kuramoto–Sivashinsky equation. Also Garcia-Ybarra & Velarde (1987) show that for a standard liquid, on heating the layer from above or cooling it from below, an interfacial instability may develop due to surface tension inhomogeneities, leading to sustained oscillations, in contrast again to our case where sustained oscillations are obtained by heating (not cooling) from below. When these sustained oscillations are forced in a nonlinear regime, then soliton-like behaviour may be expected. For a single-component layer, disregarding all matter transport and restricting the analysis to the simplest Marangoni–Bénard instability, they obtain a dispersion relation for capillary–gravity waves (Gardia-Ybarra &Velarde 1987, equations (18) and (24)) which is much more complicated than for pure capillary waves or for pure gravity waves. These relations do not look like (8), taking the form $f(\omega, k) = 0$, seemingly not easily amenable to an explicit form $\omega = f(k)$. In the limit of motions of sufficiently high frequency, on

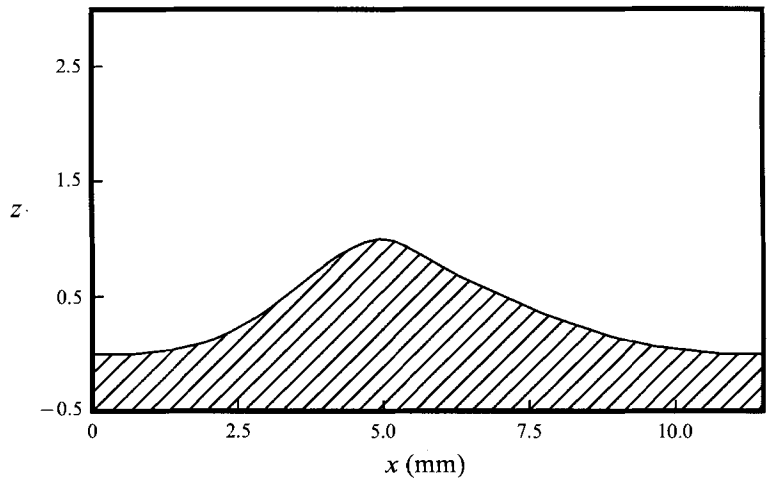

FIGURE 15. An example of a reconstructed waveform $z(x)$. Scales are arbitrary.

searching for solutions at small capillary numbers and large Marangoni numbers, the dispersion relation takes the explicit form $\omega^2 \approx k(1+k^2)$ in which we have omitted irrelevant constants (start from equation (31) in Garcia-Ybarra and Velarde 1987) which still does not look like (8). For this case, those authors show that the oscillatory interfacial instability is to be expected for negative Marangoni numbers, i.e. for standard liquids heated from above or cooled from below, in contrast again with HBEs and HWEs. Garcia-Ybarra & Velarde also quote our previous HBE results (Weill *et al.* 1985) in relation to their findings, but as we have commented several times, there are reasons to believe that this relation is not relevant because oscillatory instabilities in HWEs are obtained by heating from below. Although much work is required to elucidate the exact nature of the waves in HWEs, an interesting step will be a quantitative study of the waveforms during propagation. Preliminary observations are reported below.

5.4. *Waveforms*

We used the system described in figure 2, which, under some assumptions, permits one to deduce the shape of the surface. Let us take the laser beam arriving on the surface to be a luminous beam of diameter zero. If the surface makes an angle α with a horizontal line, the laser beam is deviated after reflection by an angle 2α. Then the displacement of the laser impact on the photodiode array is proportional to α for α small, i.e. to the derivative $\mathrm{d}z/\mathrm{d}x$ where z is the vertical location of the surface and x an abscissa parallel to the wire. If n luminous profiles are recorded at regular time intervals Δt during the passage of a wave, we obtain a sequence of derivatives $\{\mathrm{d}z/\mathrm{d}x\}_{i=1}^{n}$ from which the waveform may be reconstructed by integration.

As a typical example, figure 15 shows a waveform for silicon oil with $d = 1.28$ mm and $\Delta T = 59$ °C ($f = 1.55$ Hz, $\lambda = 11.5$ mm), propagating from right to left. We note the lack of symmetry of the wave, with a rather steep front and a smoother tail. The surface deformation cannot be represented by the usual sinusoidal waves, even with the inclusion of various numbers of harmonics, but rather looks like a wavepacket of great energy.

We emphasize that the profile in figure 15, while showing the above characteristics, concerns preliminary observations and has a strong qualitative character. It does not result from averaging several profiles. Experimental data points are not plotted because

the technique does not record the value of z defining the elevation of the wave but, rather, the slope of the surface. The accuracy of the technique is very poor and does not provide accurate numerical results. Values of z are given in arbitrary units to avoid misleading the reader with an undue impression of accuracy. We wanted to end these experimental sections with these preliminary observations from figure 15 and hope that refinements or the use of other techniques will later provide us with more quantitative results.

6. Theoretical understanding

Although this paper is devoted to new experimental results, it is now completed by a brief report concerning our present understanding of the observed phenomena: this understanding is admittedly far from fully satisfactory. We have at best at the present time the simple reductionist model, trying to include the gist of the phenomena studied, discussed by Gouesbet (1990*a*, *b*).

In this model, heat is transported from the heat source to the free surface in a characteristic time t_1, either by a diffusion-dominated mechanism or by a convection-dependent mechanism (thermal plume) depending on whether d is small or large. When the heat reaches the free surface, the warm lump of fluid is disrupted by the Marangoni effect in a characteristic time t_2. The condition $t_1 \gg t_2$ is sufficient for the process to have a cyclical character, with upward heat transfer followed by a change in surface tension and a Marangoni-induced disruption of the surface; at the same time, convective cooling occurs below. The surface disruption results in waves which propagate on the surface in the direction parallel to the wire. Conversely, if $t_1 \ll t_2$, heat is rapidly supplied to the surface and gently removed. We may then expect the appearance of a steady balance. Hence, the behaviour of the system is controlled by the value of the characteristic time ratio $R = t_1/t_2$, with a critical value $R_* = \chi$ at the onset.

With this qualitative picture in mind, the model is then developed by evaluating characteristic times, and ends with a nonlinear dynamical system in a 3D-phase space, corresponding to a coupling between a mechanical oscillator associated with the free surface and a thermal oscillator associated with the heating source. The development of the model is rather lengthy but, referring to Gouesbet (1990*a*, *b*), the following features can easily be isolated:

(i) To understand the Hopf bifurcation described in this paper, it is sufficient to consider the part of the model dealing with the free-surface mechanical oscillator and dismiss the thermal oscillator, i.e. the temperature at the heating location is assumed to be a constant. The model then develops in a 2D-phase space $(\xi, \dot{\xi})$, where ξ is the deformation of the free surface and $\dot{\xi}$ its vertical velocity.

(ii) Because Hopf bifurcation is a local bifurcation which may be understood by a linear disturbance approach, nonlinearities may be omitted in understanding the onset of oscillatory instability.

(iii) Because the characteristic time t_1 is evaluated in a different way depending on whether d is small (free surface depressed before onset of stability, conductive heat transfer) or d is large (free surface elevated, convective heat transfer), the model must involve a matching process. For simplicity, the matching is non-analytic, leading to the singular point in figure 6(*a*).

(iv) The model shows that the ratio R of characteristic times may be expressed in terms of Rayleigh and Marangoni numbers (denoted $\mathcal{N}_{Ra}$ and $\mathcal{N}_{Ma}$ in Gouesbet 1990*b*) which are therefore relevant dimensionless groups in the problem (see also Gouesbet 1987), and of four unknown elements. Furthermore, the critical value of the ratio R

cannot be predicted by the model. The model however does succeed in getting rid of the four unknown elements in such a way that the critical value $R_* = \chi$ of R may without much damage be taken equal to 1. A similar situation arises in a simple explanation of Rayleigh–Bénard instability (see Bergé *et al.* 1984, pp. 88–90) showing that the Rayleigh number is the relevant dimensionless group but without any possibility of evaluating the critical value in this simple framework. Also, in the Lorenz model for convection, the critical value of the so-called parameter R (Lorenz 1963; Thompson & Stewart 1987, chapter 11) representing the Rayleigh number is equal to 1, a value which has nothing to do with the actual value observed in experiments. In order to compare experimental data and model results, it thus emerges that the relevant dimensionless groups $\mathcal{N}_{Ra}$ and $\mathcal{N}_{Ma}$ cannot be used. The presentation which has been chosen in this paper better fits the capabilities of the simple model, as exemplified in figures 6(*a*) and 7(*a*) in which the solid lines are model results.

(v) Because unknown elements are eliminated in the model, it turns out that the characteristic times t_1 and t_2 cannot be theoretically evaluated in a proper way and therefore comparisons between experimental and theoretical characteristic times cannot be made.

(vi) When eliminating unknown elements and presenting theoretical results in a way that allows comparisons with experiments, the model dispenses with the values of the thermophysical properties of the liquids. Therefore, the model does not permit an answer to the question of whether a given liquid will or will not produce oscillatory phenomena in HBEs or HWEs. This is an unsolved problem at the present time.

7. Conclusion

New results concerning the production of oscillatory motion when a hot wire is located below an interface have been obtained with an improved version of an experimental set-up described by Weill *et al.* (1985). Instead of studying only silicon oils, the present work added to previous data by also investigating the critical quantities for the onset of oscillations in pentanol. However, the most significant extensions concern the study of the domain $(\Delta T, d)$ beyond the critical line $f(\Delta T_*, d)$ of the supercritical Hopf bifurcation, and a more systematic characterization of the wave oscillations, in particular of their dispersion relation.

The main conclusions are as follows. Reduced critical profiles for temperature differences and frequencies have been confirmed for silicon oils. The strong analogy between the present work (HWEs) and laser experiments (HBEs) in which heating is done by a laser beam rather than a hot wire is confirmed. The similarity between HWEs and HBEs still holds for volatile liquids (toluene, pentanol) but reduced profiles at the onset of instability quantitatively depart from the profiles observed for silicon oils and predicted by Gouesbet's model. This departure appears not to be attributable to mass transfer through the interface resulting from the liquid volatility, and therefore demands a new theoretical effort. The oscillations at the free surface are not directly comparable with capillary nor gravity waves, and their exact nature remains to be elucidated. In particular, they exhibit a dispersion relation for which we could find no equivalent in the literature.

The experimental observations reported in this paper and their differences with the model open the way to new experiments. Among them, we plan to repeat HWEs at high pressures to check whether secondary instabilities up to chaos may be produced as observed in HBEs. We may also supply the wire with a fixed electric current (no temperature control). Such experiments would allow the creation phase spaces of

increasing dimension by modulating the supplied intensity and/or by coupling several wires in a well-controlled way, possibly permitting evolution to the study of spatio–temporal chaos. We also note that some liquids, like water, do not produce any oscillatory phenomena: the reason why is still unknown. Last but probably not least, a systematic study of the nonlinear waves produced at the free surface is warranted to investigate whether they are solitons and, if so, of which kind. Therefore, the hot-wire experiments described in this paper probably open the way to nice new opportunities to study well-controlled spatio–temporal nonlinear dynamics and nonlinear hydrodynamic wave propagation.

REFERENCES

ANTHORE, R., FLAMENT, P., GOUESBET, G., RHAZI, M. & WEILL, M. E. 1982 A note on the interaction between a laser beam and some liquid media. *Appl. Optics* **21**, 2.

BAZHENOV, V. Y., VASNETSOV, M. V., SOSKIN, M. S. & TARANENKO, V. B. 1989*a* Self-oscillations of a liquid near a free surface during continuous local heating. *JETP Lett.* **49**, 376.

BAZHENOV, V. Y., VASNETSOV, M. V., SOSKIN, M. S. & TARANENKO, V. B. 1989*b* Dynamics of laser-induced bubble and free-surface oscillations in an absorbing liquid. *Appl. Phys.* B **49**, 485.

BERGÉ, P., POMEAU, Y. & VIDAL, C. 1984 *L'ordre dans le Chaos.* Hermann.

DEVANEY, R. L. 1987 *An Introduction to Chaotic Dynamical Systems.* Addison-Wesley.

GARCIA-YBARRA, P. L., CASTILLO, J. L. & VELARDE, M. G. 1987 Bénard–Marangoni convection with a deformable interface and poorly conducting boundaries. *Phys. Fluids* **30**, 2655.

GARCIA-YBARRA, P. L. & VELARDE, M. G. 1987 Oscillatory Marangoni–Bénard interfacial and capillary–gravity waves in single- and two-component liquid with or without Soret thermal diffusion. *Phys. Fluids* **30**, 1649.

GOUESBET, G. 1987 New presentation of experimental results for overstability phenomena produced by a hot-wire located near and below a free surface. *Phys. Chem. Hydrodyn.* **8**, 349.

GOUESBET, G. 1990*a* Dynamical states and bifurcations in a new thermo-dynamical system: optical heartbeats and associated phenomena. *Entropie*, no. 153/154.

GOUESBET, G. 1990*b* Simple model for bifurcations ranging up to chaos in thermal lens oscillations and associated phenomena. *Phys. Rev.* A **41**, 5928.

GOUESBET, G. & LEFORT, E. 1987 Thermal lens oscillations at low laser powers. *Appl. Optics* **26**, 2940.

GOUESBET, G. & LEFORT, E. 1988 Dynamical states and bifurcations of a thermal lens using spectral analysis. *Phys. Rev.* A **37**, 4903.

GOUESBET, G. & MAQUET, J. 1989 Examination of an analogy toward the understanding of thermal lens oscillations. *AIAA J. Thermodyn. Heat Transfer* **3**, 27.

GOUESBET, G., MAQUET, J., ROZÉ, C. & DARRIGO, R. 1990 Surface tension- and coupled buoyancy-driven instability in a horizontal liquid layer. Overstability and exchange of stability. *Phys. Fluids* A **2**, 903.

GOUESBET, G., RHAZI, M. & WEILL, M. E. 1983 A new heart-beating phenomenon and the concept of 2D-optical turbulence. *Appl. Optics* **22**, 304.

GOUESBET, G., ROZÉ, C. & MAQUET, J. 1992 Overstability in an infinite liquid layer under simultaneous surface tension, buoyancy and shear effects. *Proc. Intl Symp. on Instabilities in Multiphase Flows, Rouen, May 11–14, 1992.* (In press.)

GOUESBET, G. & SUKHODOL'SKII, A. T. 1992 Opportunity of investigation of fluid interface instability and solar thermocapillarity phenomena in space. In *Hydrodynamics and Heat/Mass Transfer in Microgravity*, pp. 331–334. Gordon and Breach.

GOUESBET, G., WEILL, M. E. & LEFORT, E. 1986 Convective and free surface instabilities provoked by heating below an interface. *AIAA J.* **24**, 1324.

GUCKHENHEIMER, J. & HOLMES, P. 1983 *Nonlinear Oscillations, Dynamical Systems and Bifurcations of Vector Fields.* Springer.

JOSEPH, D. D. 1976 *Stability of Fluid Motions.* Springer.

KAYSER, W. V. & BERG, J. C. 1973 Surface relief accompanying natural convection in liquid pools heated from below. *J. Fluid Mech.* **57**, 739.

LANDAU, L. & LIFSHITZ, E. 1971 *Mécanique des Fluides.* Moscow: MIR Editions.

LORENZ, E. N. 1963 Deterministic nonperiodic flow. *J. Atmos. Sci.* **20**, 130.

MAQUET, J., GOUESBET, G. & BERLEMONT, A. 1967 A computer code for natural convection in an enclosed cavity with a free surface. In *Proc. Intl Conf. Numerical Methods in Thermal Problems*, vol. 5, part I (ed. R. W. Lewis, K. Morgan & W. G. Habashi), pp. 472–483. Swansea: Pineridge.

MEUNIER-GUTTIN-CLUZEL, S. 1990 Caractérisations et modélisations des régimes chaotiques de la lentille thermique. Thèse de doctorat, Université de Rouen.

PARANTHOËN, P. & PETIT, C. 1979 Influence de la conduction entre le capteur et ses supports sur la mesure des fluctuations de température dans un écoulement turbulent effectué à l'aide d'un thermomètre à résistance. *Lett. Heat Mass Transfer* **6**, 311.

PEREZ-GARCIA, C. & CARNEIRO, G. 1991 Linear stability analysis of Bénard–Marangoni convection in fluids with a deformable free surface. *Phys. Fluids* A **3**, 292.

REIMAN, J. 1973 Experimental investigation of free convection flow from wires in the vicinity of phase interfaces. *Intl J. Heat Mass Transfer* **17**, 1051.

ROZÉ, C., GOUESBET, G. & MAQUET, J. 1990 Overstability under simultaneous surface tension, buoyancy and shear effects in a horizontal liquid layer. *28th AIAA Aerospace Sciences Meeting, 8–11 January 1991, Reno, USA.*

SCHORR, A. W. & GEBHART, B. 1970 An experimental investigation of natural convection wakes above a line heat source. *Intl J. Heat Mass Transfer* **13**, 557.

TAKASHIMA, M. 1981*a* Surface tension driven instability in a horizontal liquid with a deformable free surface. I. Stationary convection. *J. Phys. Soc. Japan* **50**, 2745.

TAKASHIMA, M. 1981*b* Surface tension driven instability in a horizontal liquid with a deformable free surface. II. Overstability. *J. Phys. Soc. Japan* **50**, 2751.

THOMPSON, J. M. T. & STEWART, H. B. 1987 *Nonlinear Dynamics Systems and Chaos.* John Wiley and Sons.

VIZNYUK, S. A. & SUKHODOL'SKII, A. T. 1988 Capillary–gravity instability of fluid motion with continuous laser heating. *Sov. Phys. Tech. Phys.* **33**, 609.

WEILL, M. E., RHAZI, M. & GOUESBET, G. 1982 Oscillations d'une surface libre chauffée sous l'interface à l'aide d'un fil. *C.R. Acad. Sci. Paris* **294**, 567.

WEILL, M. E., RHAZI, M. & GOUESBET, G. 1985 Experimental investigation of oscillatory phenomena produced by a hot-wire located near and below a free surface. *J. Phys. Paris* **46**, 1501.

ZIEREP, J. & OERTEL, H. (Ed.) 1982 *Convective Transport and Instability Phenomena.* Karlsruhe: Braun.